Adatom-assisted structural transformations of fullerenes

In-Ho Lee, Sukky Jun, Hanchul Kim, Sung Youb Kim, and Youngmin Lee

---

Articles you may be interested in

Synthesis, characterizations, and thermal induced structural transformation of silver-fullerene C 60 nanocomposite thin films for applications in optical devices
J. Appl. Phys. **107**, 103504 (2010); 10.1063/1.3366709

Structural changes and catalytic activity of platinum nanoparticles supported on C 60 and carbon nanotube films during the operation of direct methanol fuel cells
Appl. Phys. Lett. **88**, 073113 (2006); 10.1063/1.2177354

Enhanced strain relaxation rate of InGaAs by adatom-assisted dislocation kink nucleation
J. Vac. Sci. Technol. B **23**, 1166 (2005); 10.1116/1.1914823

Structure and dynamics of endohedral fullerenes
AIP Conf. Proc. **544**, 131 (2000); 10.1063/1.1342484

Structure and microhardness of low pressure polymerized fullerite C 60
Low Temp. Phys. **24**, 896 (1998); 10.1063/1.593524

Adatom-assisted structural transformations of fullerenes

In-Ho Lee[a)]
Korea Research Institute of Standards and Science, Daejeon 305-600, Korea

Sukky Jun
Department of Mechanical and Materials Engineering, Florida International University, Miami, Florida 33174

Hanchul Kim
Korea Research Institute of Standards and Science, Daejeon 305-600, Korea

Sung Youb Kim and Youngmin Lee
Department of Mechanical Engineering, Korea Advanced Institute of Science and Technology, Daejeon 305-701, Korea

Microscopic mechanism of autocatalytic structural transformations of fullerenes is investigated by the action-derived molecular dynamics. Dynamic pathways and the corresponding activation energies are obtained for the Stone-Wales transformation in fullerene and the fullerene coalescence, under the presence of extra carbon atoms. The adatom-assisted Stone-Wales transformation is proved to be a highly probable process unit for the structural transformations and annealing treatments of carbon-based graphitic networks. The complex processes of adatom-assisted fullerene coalescence, yielding very low activation energies, are presented. © *2006 American Institute of Physics*. [DOI: 10.1063/1.2161175]

Understanding the mechanism of autocatalytic reaction is of great importance for the precise synthesis of various carbon nanostructures. For example, a recent experiment has revealed that the polymerization of C_{60} fullerenes in a peapod proceeded slowly to build an inner single-walled carbon nanotube at the temperature of 800 °C.[1] From their experiments using Raman scattering and 120 kV transmission electron microscopy, it was deduced that several carbon atoms could be released from the carbon network and move around inside the tube. Consequently, such migrating carbon atoms were likely to be taken into the polymerization of neighboring fullerenes and to cause a drastic decrease in the activation barrier for structural relaxation.[1]

In addition, low-energy electron irradiations and gas-phase depositions have widely been discussed as the sources of extra carbon atoms that can possibly participate in the structural transformations of carbon fullerenes.[1–5] Extra carbon atoms are thus believed to play an important role in the fullerene coalescence inside a carbon nanotube. However, it is extremely difficult to experimentally explore autocatalytic reactions with spatial and temporal resolutions sufficient to observe its microscopic mechanism.[6]

The roles of a carbon adatom have been theoretically studied for the Stone-Wales (SW) transformation in graphite networks[2,3,7] because the SW-like bond rotation is the key process unit generally applicable to various structural transformations. It has been reported that the presence of the adatom could reduce the energy barrier considerably.[2,3,7] In contrast to these statics-based energy calculations, we here present *dynamic* pathway models for adatom-assisted structural transformations of fullerenes.

Microscopic-level mechanism of the motion of extra carbon atoms is provided by constructing the atomic trajectory connecting two given atomic configurations, i.e., a reactant and a product, respectively, where the extra carbon atoms and fullerenes are sufficiently apart in order not to interact with each other, i.e., $C_{60}+C_{60}+C \rightarrow C_{120}+C$, for example. Our results strongly support the experimental observations such as exchanges of extra carbon atoms during the process of autocatalysis.[8]

For the pathway construction, we discretized and minimized the modified classical action including both the restraint of total-energy conservation and the control of kinetic energy together within the framework of action-derived molecular dynamics (ADMD).[9–11] The interaction between carbon atoms were described by the interatomic potential based on tight-binding method.[12] Due to the general importance of SW-like defects formation as mentioned earlier, we begin our simulations with the autocatalytic SW transformation in a C_{60} molecule. Next, following is the autocatalytic coalescence of fullerenes, i.e., the fusion from two C_{60} fullerenes into a C_{120} molecular capsule in the presence of extra carbon atoms.

We first simulated the uncatalyzed SW transformation where the initial conformation was a defect-free C_{60} and the final one was the C_{60} containing a SW defect. The total simulation time of 1.2 ps was discretized by 200 intervals so that each time increment between adjacent steps was 6.0 fs. For each numerical example, both initial and final conformations were fully relaxed via finding local minima of potential energy, before performing its ADMD simulations. The activation energy barrier E_a is defined by the difference between the highest potential energy during the whole process and the potential energy of the initial atomic conformation. For the uncatalyzed SW transformation, we obtained $E_a=5.9$ eV.

For the autocatalytic SW transformation in a C_{60}, we simulated a number of different cases according to the presumed route of an extra atom passing by the C_{60}. Some of them were devoted to the situations that the extra carbon

---
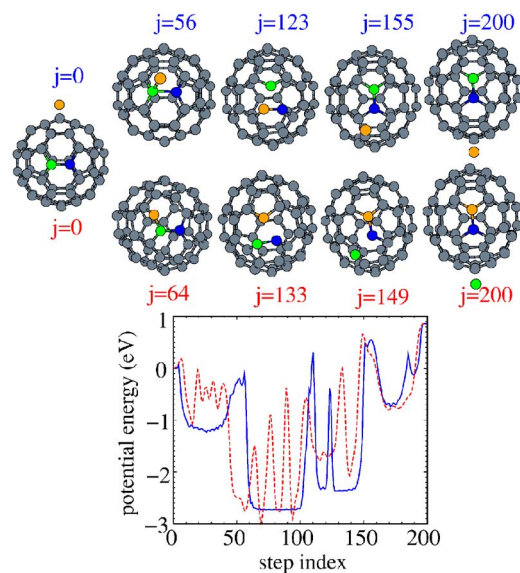
a)Electronic mail: ihlee@kriss.re.kr

FIG. 1. (Color online) Autocatalytic SW defect formations in a C_{60} are simulated by the ADMD method. Initial, intermediates, and final conformations with the corresponding step indices are shown for two different pathways (with and without exchange). Potential-energy plots, corresponding to each pathway, are shown in the lower part.
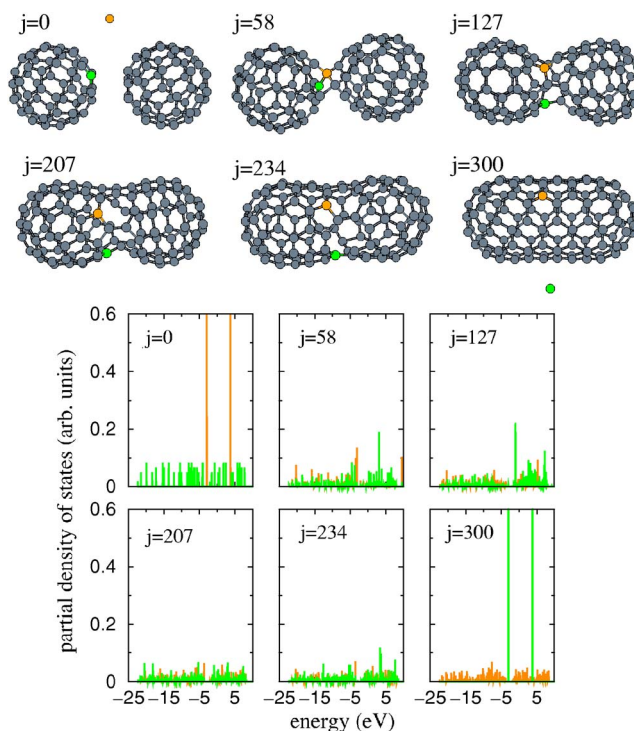

FIG. 2. (Color online) Six snapshots with step indices are shown for the autocatalytic fullerene fusion with exchange. The development of partial density of states associated is also given in the lower part.

atom is passing by the C_{60}, whereas others were for the cases that it is escaping out from the inside of the fullerene. In the initial and final conformations of all cases, the extra atom was placed far from each atom of C_{60} so that we could neglect its interaction with the C_{60} molecule. The activation energies obtained from our numerical experiments ranges from 0.9 to 3.4 eV. We have also performed the case that the extra carbon atom exchanges its position with an atom of the C_{60} molecule. Among many cases, two representative results of ADMD simulation for autocatalytic SW transformations are compared in Fig. 1. Both cases share the same initial configuration, but the final configurations are different from each other. In the upper case, the incoming extra carbon atom (in orange color) comes out after completing the SW transformation, while the exchange of carbon atoms takes place in the lower case. The potential-energy variations of both pathways are also shown in the lower part of Fig. 1.

The activation energies of both pathways are 0.9 eV, while 5.9 eV is obtained for the uncatalyzed SW transformation in a C_{60} fullerene as mentioned earlier. This value of 0.9 eV is the same as the potential-energy difference between the initial and final states, i.e., the fully relaxed C_{60} fullerenes with and without a SW defect. Within the framework of ADMD, the initial and final conformations are totally interchangeable, which implies the microscopic reversibility of reaction pathways.[9] As a result, these pathways are barrierless in time reversal, and accordingly provide a natural microscopic event for understanding the fullerene annealing processes. The barrierless pathway models can also be applied to the annealing treatments for the growth and structural change of various carbon nanostructures because the SW rotation is an essential phase in the generic structural transformations of the graphitic network.

As our next numerical experiment of autocatalytic reaction, the fusion process was considered under the participation of one extra carbon atom or two. The centers of two fullerenes were initially separated by 9.9 Å away from each other.[4] A C_{120} capsule of (5,5) nanotube chirality was se-

lected as the product in final configurations. The total simulation time was 1.8 ps. It was discretized by 300 intervals and each time increment was thus 6.0 fs. In Fig. 2, six snapshots of an autocatalytic process are presented. The initial and final positions of the extra carbon atom were chosen such that its presumed path goes through the midzone of coalescence between the two fullerenes. For this specific example, we also assumed that the catalytic atom was exchanged; that is, the incoming and outgoing atoms are not identical. The activation energy barrier of 1.1 eV is obtained for this exchange case, which is lower than that without exchange (1.4 eV). Therefore, our results agree with the experiment that the exchange is more likely as suggested from experiments.[8]

To understand the electronic effects on the catalytic reaction, we investigated the partial density of states associated with adatoms as shown in the lower part of Fig. 2. The localized electronic states associated with nonbonded adatoms are clearly shown in the initial and final conformations, as expected. According to the extent of chemical bonds between the adatom and the intermediate conformations of carbon molecules, the variation of the partial density of states can easily be noticed. The bonding character of the adatom during the catalytic reaction is ranging from sp bonding to $sp2$ bonding. In Fig. 2, at the step indices 207 and 234, both atoms in orange and in green reveal the $sp2$ bonding character. Other conformations ($j=58$ and $j=127$), except the ones containing nonbonded adatom, show the sp bonding character which is usually found in carbon chain and carbyne.

It is of special note that the adatom-assisted reduction of activation energy is mainly made during the former half among the whole process. That is, the adatom effectively participates in the early bond-breaking and rebonding stages by capturing the dangling bonds or forming sp or $sp2$ bonds
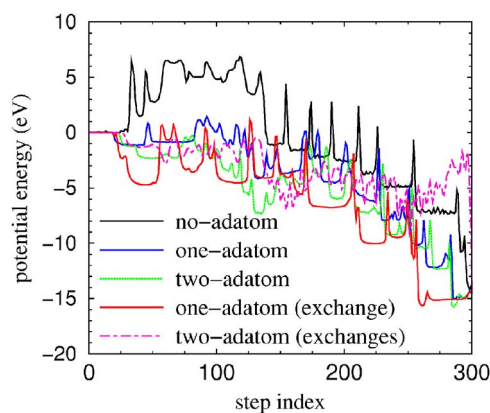
FIG. 3. (Color online) Simulated potential-energy variations are shown for five different dynamic pathways of fusion, $C_{60}+C_{60}\rightarrow C_{120}$. One-adatom and two-adatom imply the cases of autocatalytic reaction, and exchange denotes the case that the incoming and outgoing carbon atoms are not identical.

locally. As shown in Fig. 2, the extra atom are going toward the merging region, and are actively assisting the structural transformations inside the peanut-like intermediate shapes. We observed that, in the early part of uncatalyzed process, several bond-breaking and rebonding steps, costing high energy, take place in order to open the two cages and then to begin joining them. On the other hand, after shaping the peanut-like intermediate, successive SW-like bond rotations are needed to complete the perfect form of C_{120} nanocapsule. These SW-like bond rotation are recognized by the sharp peaks in the latter half of the potential-energy plot given in Fig. 3.

The active contributions of adatoms were easily found by comparing the activation energy barriers. As shown in Fig. 3, the activation energy barrier of 6.8 eV was obtained for the uncatalyzed case, whereas 0.0– 1.4 eV for autocatalytic pathways which are the cases of one adatom, two adatoms, one adatom with exchange, and two adatoms with exchanges, respectively. The adatoms effectively participate in the early bond-breaking and rebonding stages by capturing the dangling bonds or forming sp or $sp2$ bonds locally, which effectively reduces the activation energy to overcome.

The autocatalytic fusion process is energetically more favorable than the vacancy-driven fusion process which has to overcome much higher activation energy barrier.[1] This is based on the fact that a C–C bond breaking requires ~3 eV. The high possibility of the autocatalytic fullerene fusion can be supported by the low activation energy of ~0.8 eV for carbon adatoms to migrate inside single-walled carbon nanotubes proposed both experimentally and theoretically.[13,14] The deduction of adatom drift was also drawn from the recent C_{60} fusion-induced nanotube synthesis at the temperature of 800 °C as stated earlier.[1] Low activation barriers obtained from ADMD calculations thus support the recent experimental observations which inferred the role of extra carbon atoms as well as the exchange of the catalytic carbon atoms.[1,8] Our dynamic pathway models further provide a theoretical foundation such that the coalescing process of fullerenes in a nanopeapod can easily be activated by injecting the low-energy flux of carbon ions. In experiment, extra carbon atoms may also be generated by the knock-on effect induced by electron irradiations.[13]

[1]S. Bandow, T. Hiraoka, T. Yumura, K. Hirahara, H. Shinohara, and S. Iijima, Chem. Phys. Lett. **384**, 320 (2004).
[2]B. R. Eggen, M. I. Heggie, G. Jungnickel, C. D. Latham, R. Jones, and P. R. Briddon, Science **272**, 87 (1996).
[3]C. P. Ewels, M. I. Heggie, and P. R. Briddon, Chem. Phys. Lett. **351**, 178 (2002).
[4]B. W. Smith, M. Monthioux, and D. E. Luzzi, Nature (London) **396**, 323 (1998).
[5]B. W. Smith and D. E. Luzzi, Chem. Phys. Lett. **321**, 169 (2000).
[6]P. M. Ajayan, Nature (London) **427**, 402 (2004).
[7]P. Jensen, J. Gale, and X. Blase, Phys. Rev. B **66**, 193403 (2002).
[8]J. F. Christian, Z. Wan, and S. L. Anderson, J. Phys. Chem. **96**, 3574 (1992).
[9]D. Passerone and M. Parrinello, Phys. Rev. Lett. **87**, 108302 (2001).
[10]I.-H. Lee, J. Lee, and S. Lee, Phys. Rev. B **68**, 064303 (2003).
[11]I.-H. Lee, H. Kim, and J. Lee, J. Chem. Phys. **120**, 4672 (2004).
[12]C. H. Xu, C. Z. Wang, C. T. Chan, and K. M. Ho, J. Phys.: Condens. Matter **4**, 6047 (1992).
[13]F. Banhart, Rep. Prog. Phys. **62**, 1181 (1999).
[14]A. V. Krasheninnikov, K. Nordlund, P. O. Lehtinen, A. S. Foster, A. Ayuela, and R. M. Nieminen, Phys. Rev. B **69**, 073402 (2004).